The effect of single-ossicle ear flexibility and eardrum cone orientation on quasi-static behavior of the chicken middle ear

The effect of single-ossicle ear flexibility and eardrum cone orientation on quasi-static behavior of the chicken middle ear

Pieter G.G. Muyshondt[a,1], Peter Aerts[b,c], Joris J.J. Dirckx[a]

[a] *University of Antwerp, Biophysics and Biomedical Physics, Groenenborgerlaan 171, 2020 Antwerp, Belgium*

[b] *University of Antwerp, Functional Morphology, Universiteitsplein 1, 2610 Antwerp, Belgium*

[c] *University of Ghent, Department of Movement and Sport Science, Watersportlaan 2, 9000 Ghent, Belgium*

[1] *E-mail address:* pieter.muyshondt@uantwerpen.be

Abstract

In the single-ossicle ear of chickens, the quasi-static displacement of the umbo shows great asymmetry; umbo displacements are much larger for negative than for positive pressure in the middle ear, which is opposite to the typical asymmetry observed in mammal ears. To better understand this behavior, a finite-element model was created of the static response of the chicken middle ear. The role of flexibility of the extracolumella in the model was investigated, and the potential effect of the outward orientation of the tympanic-membrane cone was studied by building two adapted models with a flat membrane and an inverted conical membrane. It is found that the extracolumella must be made of flexible material to explain the large inward displacements of the umbo, and that displacements of the footplate are much smaller due to bending of the flexible extracolumella. However, increasing extracolumellar stiffness mostly reduces umbo displacement rather than increasing footplate displacement. The results suggest that the inverted orientation of the membrane cone is responsible for the change in asymmetry of the umbo displacement curve. The asymmetry of the footplate displacement curve in the normal model is smaller, but increases towards positive middle-ear pressure in the case of a flat or inverted membrane geometry.

Keywords

Bird middle ear – finite-element modeling – quasi-static pressure – tympanic membrane – (extra)columella

Highlights

- Quasi-static middle-ear behavior in chicken was studied by finite-element modeling
- The flexible extracolumella permits large inward eardrum displacements
- Flexibility of the extracolumella affects umbo motion rather than footplate motion
- Inverting the eardrum may lead to opposite asymmetry of avian umbo displacements

1. Introduction

Birds are one of the classes of vertebrates that have ears with a single ossicle. This type of ear is of interest to clinicians and researchers who are developing new middle-ear prostheses, because it possesses two important properties that a well-functioning single-ossicle ear should have: the ability to efficiently transmit sound from the outer ear to the inner ear, and the flexibility to manage large quasi-static pressure changes between the middle-ear and the environment (Mason and Farr, 2013).

The single ossicle of birds – the bony columella – is coupled to the tympanic membrane by the more flexible extracolumella, which is a tripod that is composed of hyaline cartilage. Similar to mammals, the tympanic membrane in birds has a curved conical shape. However, in birds the tip of the cone points outwards, that is, in the direction opposite to what is typically seen in mammals. The avian tympanic membrane is pushed into the ear canal by the central arm of the extracolumella – the extrastapedius.

Studies of the quasi-static performance of the avian middle ear are scarce. In anatomical analyses and other studies using structural manipulations or quasi-static pressure variations to deform the tympanic membrane, the connection between the columella and extracolumella was identified as a zone of compliance (Smith, 1904; Pohlman, 1921; Norberg, 1978; Starck, 1995; Mills and Zhang, 2006; Arechvo et al., 2013). A recent study investigated quantitative umbo and footplate displacements and tympanic-membrane deformations in the chicken when the middle ear was exposed to static pressure changes from –1.5 to +1.5 kPa relative to atmospheric pressure (Claes et al., 2018). The observed displacements showed a nonlinear behavior as a function of middle-ear pressure, and the displacement curves were asymmetric; umbo and footplate displacements were larger at negative than positive static middle-ear pressure, which is opposite to the asymmetry observed in mammal ears (Hüttenbrink, 1988; Dirckx and Decraemer, 1991 & 2001; Dirckx et al., 2006). Also measurements of tympanic-membrane volume displacement in human have shown larger values at positive than negative static middle-ear pressure (Elner et al., 1971; Dirckx and Decraemer, 1992). The large umbo displacements at negative middle-ear pressure in chicken were accompanied with bending of the extracolumella, leading to much smaller displacements at the columellar footplate, which may offer protection to the inner ear.

In the present work, finite-element modeling is used to better understand the observed quasi-static displacements of the umbo and footplate in the chicken, and how this behavior is related to the shape and orientation of the tympanic-membrane cone and the flexibility of the components in the columellar apparatus.

2. Materials and methods

2.1 Finite-element modeling

2.1.1 Model geometry

The geometry of the model was based on a micro-CT scan of a fresh dissected left ear of a female chicken. The sample was unstained to avoid shrinkage of soft tissue (Buytaert et al., 2014) and any possible changes in tympanic-membrane shape. The sample was wrapped in thin plastic film (Parafilm, Bemis NA, Neenah, WI, USA) to avoid dehydration during scanning. The scan was performed using a Skyscan 1172 micro-CT scanner (Bruker, Kontich, Belgium) located at the VUB in Brussels, Belgium. The scan was made using a source voltage of 79 kV and source current of 125 µA. The total scan time comprised 2 hours and 4 minutes for an image acquisition over 360 degrees. The reconstructed image data set had a size of 2000x2000x1246 pixels and a voxel size of 10.9 µm, and contained no overlap between slices.

Subsequently, image segmentation was performed in Amira 6.3 (FEI, Hillsboro, OR, USA) to identify the different ME components. Segmentation was performed semi-automatically, combining thresholding techniques with manual segmentation to correctly identify the boundaries between different structures and the outlines of thin structures such as the tympanic membrane. The segmented data set was converted into a closed surface model built up of triangles. Smoothing operations were performed on the segmentation and surface model to remove sharp features induced by noise in the scan and the segmentation procedure.

The geometry of the middle-ear model is shown in Fig. 1 (a) and contains the following structures: the tympanic membrane, the ascending ligament, the extracolumella, the columella, the annular ligament of the columella, Platner's ligament, and the infrastapedial membrane. The extracolumella has three arms: the infrastapedius, extrastapedius and suprastapedius, as indicated in Fig. 1 (a). The distal tip of the extrastapedius, which forms the conical tip of the tympanic membrane, will be denoted as the umbo. The middle-ear muscle, of which the tendon attaches to the rim of the tympanic membrane, was not included as a separate structure in the model as it was not the aim to investigate the effect of muscle contractions. Drum-tubal ligaments which attach to the tympanic membrane were also not included in the model. To give an idea about the quality of the micro-CT data and the segmentation, a raw 2D slice of the CT reconstruction is shown in Fig. 1 (b), containing the segmented parts of several middle-ear components. The average thickness of the tympanic membrane was 33.2 µm. Only in a few small regions, the membrane thickness was close to the resolution of the scan (10.9 µm).

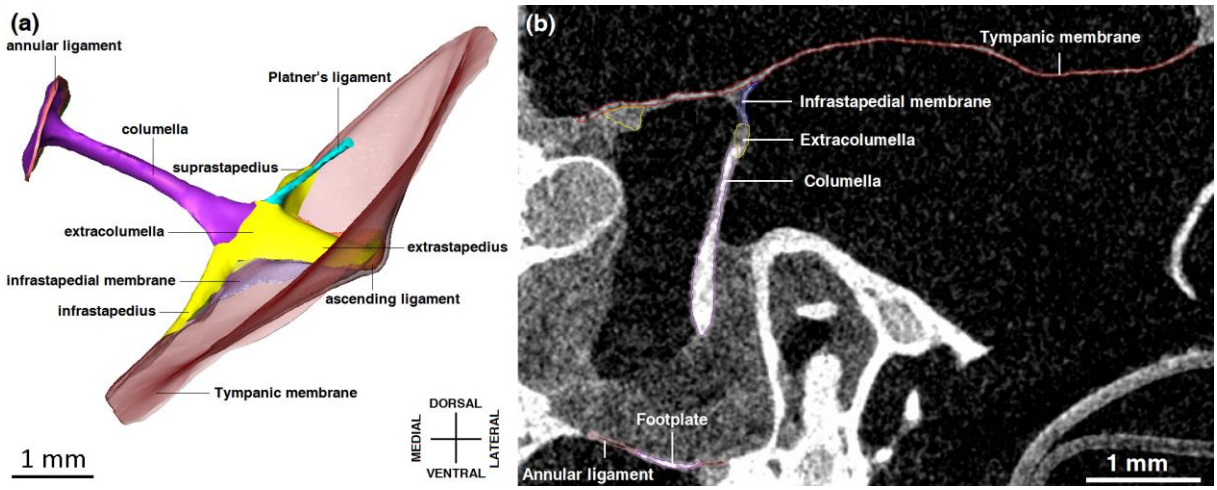

Figure 1. (a) Anterior view of the left middle ear of the chicken, used as geometry of the finite-element model. The different components of the middle ear are indicated. The tympanic and infrastapedial membrane are shown in transparent. (b) Single slice of the micro-CT reconstruction (arbitrary viewing direction). The segmented parts of some components are outlined and indicated.

2.1.2 Model description

The surface model was imported as STL file (Surface Tessellation Language) in the commercial finite-element solver COMSOL, version 5.3a (COMSOL Multiphysics, Burlington, MA, USA). The model used quadratic tetrahedral solid elements for all structures. For the tympanic membrane a single layer of tetrahedral elements was used. This description gave an umbo displacement with a relative difference of smaller than 1.2% as when a shell description was used in a model of the membrane alone. A mesh convergence analysis on the full model resulted in a relative error of smaller than 0.15% for the maximal umbo displacement between the two finest mesh resolutions. The total number of degrees of freedom resulting from this analysis was equal to 215,580.

As a boundary condition, the periphery of the tympanic membrane and the annular ligament of the columella were fixed at the boundary elements forming the periphery. As the connection of the middle-ear muscle tendon to the rim of the membrane is considered a passive constraint, this part of the rim was also modeled as fixed. Also the boundary elements at the outer end of Platner's ligament were fixed. No pressure loading related to the inner-ear fluid was imposed on the inner surface of the footplate, as it was shown in ostrich that the inner ear has no important effect on quasi-static footplate displacements (Muyshondt et al., 2016b).

Static deformations in the model were induced by applying uniform static pressures to the outer tympanic-membrane surface, with values ranging from –1.5 to +1.5 kPa as used in Claes et al. (2018). In the experiments of Claes et al. (2018), however, static pressures were applied and measured inside the middle-ear cavity. In

contrast to pressure stimulation from the ear-canal side, this approach provided the net drive of the tympanic membrane without the need to consider the compliance of the closed cavity. As we compare our model results with these measurements, no additional compliance of the middle-ear cavity was included in the model. Presumably, such a compliance will have little effect on the quasi-static behavior of the chicken middle ear. The compliance of the cavity is proportional to its volume (e.g., Motallebzadeh et al., 2017). In birds, this volume is large compared to the volume displacement of the tympanic membrane as the middle-ear cavities are pneumatically connected to a large airspace in the skull (e.g., Larsen et al., 2016). Such a large volume, and hence compliance, will only introduce a small closed-cavity pressure when compared to the isolated middle-ear cavities in mammals.

To calculate middle-ear deformations, only geometric nonlinearities of the middle-ear components were taken into account. Material nonlinearities of the tympanic membrane and other soft tissues may be important to determine accurate quantitative deformations of the middle ear, but the objective of the present work is to study the effect of the shape of the tympanic membrane on middle-ear deformations, and to investigate to what extent these properties are able to describe the experimental data.

Calculations were performed on a personal computer (Intel(R) Xeon(R) CPU E5-2630 v3, 2.40 GHz (2 processors), and 128 GB of RAM). The calculation time for a pressure sweep from –1.5 to +1.5 kPa, using pressure steps of maximally 50 Pa, was equal to 48 minutes for the normal model. The software made use of a MUMPS solver, and a Newtonian approach was applied to solve the nonlinear system of algebraic equations.

2.1.3 Material properties

For all middle-ear components, homogeneous and isotropic material properties were used. Values of these parameters, including the elastic Young's modulus E, Poisson's ratio ν and mass density ρ, are listed in Table 1. Damping was not included as we are studying static behavior of the middle ear. Mass densities and Poisson's ratios were based on values that are frequently used for soft tissue and bone in middle-ear modeling (Kirikae, 1960; Maftoon et al., 2015). Values of Young's moduli were more uncertain. The Young's modulus of the columella and Platner's ligament, to which the duck middle-ear response was shown to be less sensitive (Muyshondt et al., 2016a), were chosen based on values in other finite-element models. For the tympanic membrane and the infrastapedial membrane, a combined Young's modulus value was used that resulted in a good agreement between the model and the experimental data. The same was done for the Young's modulus of the ascending ligament and the extracolumella. The chosen value of the Young's modulus of the annular

ligament was much lower, which was of the same order as experimental estimations of the same parameter in the ostrich (Muyshondt et al., 2018). Because a-priori values of Young's moduli of these soft tissues are uncertain, a sensitivity analysis was performed on the model. To test the sensitivity of the model displacements to the Young's modulus of each individual soft-tissue component, the model was evaluated after multiplying the original modulus of that particular component by a factor of 10, while keeping the moduli of all other structures at their base value.

Table 1. Material parameter values used in the finite-element model. *E*, Young's modulus; ρ, mass density; *v*, Poisson's ratio. The Young's moduli for the remaining middle-ear components was manually adjusted within realistic bounds until the model gave the best match with the experimental data of Claes et al. (2018).

Component	*E* (MPa)	ρ (10^3 kg/m^3)	*v*
Columella	14100[a]	2.2[c]	0.3[d]
Platner's ligament	21[b]	1.1[d]	0.49[d]
Annular ligament	0.05	1.1[d]	0.49[d]
Tympanic membrane	1	1.1[d]	0.49[d]
Infrastapedial membrane	1	1.1[d]	0.49[d]
Ascending ligament	3	1.1[d]	0.49[d]
Extracolumella	3	1.1[d]	0.49[d]

References: [a] Herrmann and Liebowitz (1972), [b] Thomassen et al. (2007), [c] Kirikae (1960), [d] Maftoon et al. (2015).

The tympanic membrane was modeled as an isotropic structure. In reality, the central layer of the chicken tympanic membrane contains radially and non-radially oriented fibers, but the non-radial fibers have a very different distribution density and orientation in different parts of the membrane (Filogamo, 1949; see Fig. 13), which represents a much more irregular pattern than the composition of circumferentially organized fibers in the human tympanic membrane. Therefore, an orthotropic description with only two distinct elastic moduli, that is, in the radial and circumferential directions, would not be appropriate in the chicken. The isotropic description, as was used here, proved to be sufficient to describe the experimental behavior to a certain extent (see further).

The intracolumellar connection between the columella and extracolumella was not modeled as a separate structure in the model. Although it is regularly considered as a point of flexibility in the avian middle ear (Smith, 1904; Pohlman, 1921; Norberg, 1978; Starck, 1995; Mills and Zhang, 2006; Arechvo et al., 2013), it is no real physical joint. In ostrich it was identified as a junction zone between bone of the columella and cartilage of the extracolumella (Arechvo et al., 2013).

2.1.4 Orientation of the tympanic-membrane cone

To study the effect of the orientation of the cone of the tympanic membrane, two additional models were created with modified middle-ear geometries. In the first model the tympanic membrane was made flat, and in the second model the cone of the tympanic membrane was inverted, so that the tip of the membrane cone pointed inwards, similar to mammals. These geometries were created by prescribing a deformation to the membrane in the original finite-element model that leads to the flat and inverted membrane shape, respectively. In this procedure, the other components of the middle ear were allowed to displace and deform along with the tympanic membrane to obtain a suitable connection between the deformed structures. The only restriction was that the angle between the long axis of the columella and the base plane of the tympanic membrane is preserved. The two resulting geometries were used as input to calculate the static middle-ear behavior in the same way as described in section 2.1.2 for the normal middle-ear geometry. Note that stresses and strains caused by the deformation procedure in the model were released before performing analyses on the modified models. The original and modified middle-ear geometries are shown in Fig. 2. For the geometries with the flat and inverted tympanic membrane it can be seen that the columellar shaft and the extrastapedius are no longer oriented along the same longitudinal axis, and the difference in orientation is the greatest for the geometry with inverted tympanic membrane.

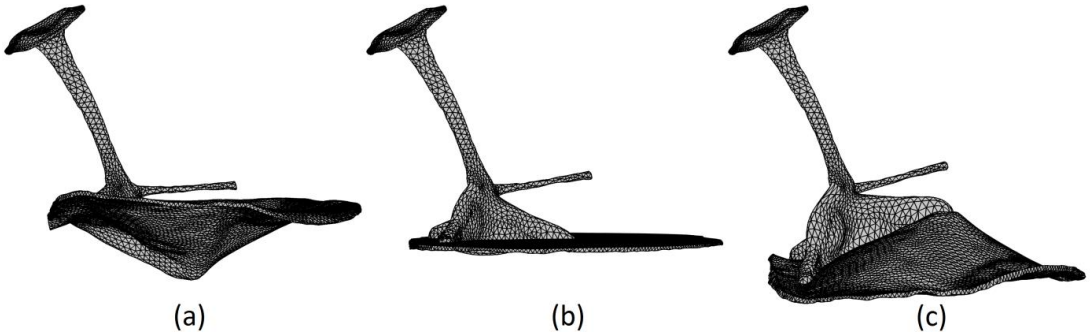

Figure 2. Ventro-anterior view of the original and modified 3D geometries of the chicken middle-ear model. (a) Geometry of the normal middle ear with the conical tip of the tympanic membrane pointing outwards. (b) Modified geometry of the middle ear with a flat tympanic membrane. (c) Modified geometry of the middle ear with an inverted tympanic membrane with the conical tip pointing inwards, similar to the membrane in mammals.

3. Results

3.1 The normal middle ear

3.1.1 Umbo and footplate displacement

The results of umbo and footplate displacement for the model with normal tympanic membrane are shown in Fig. 3.

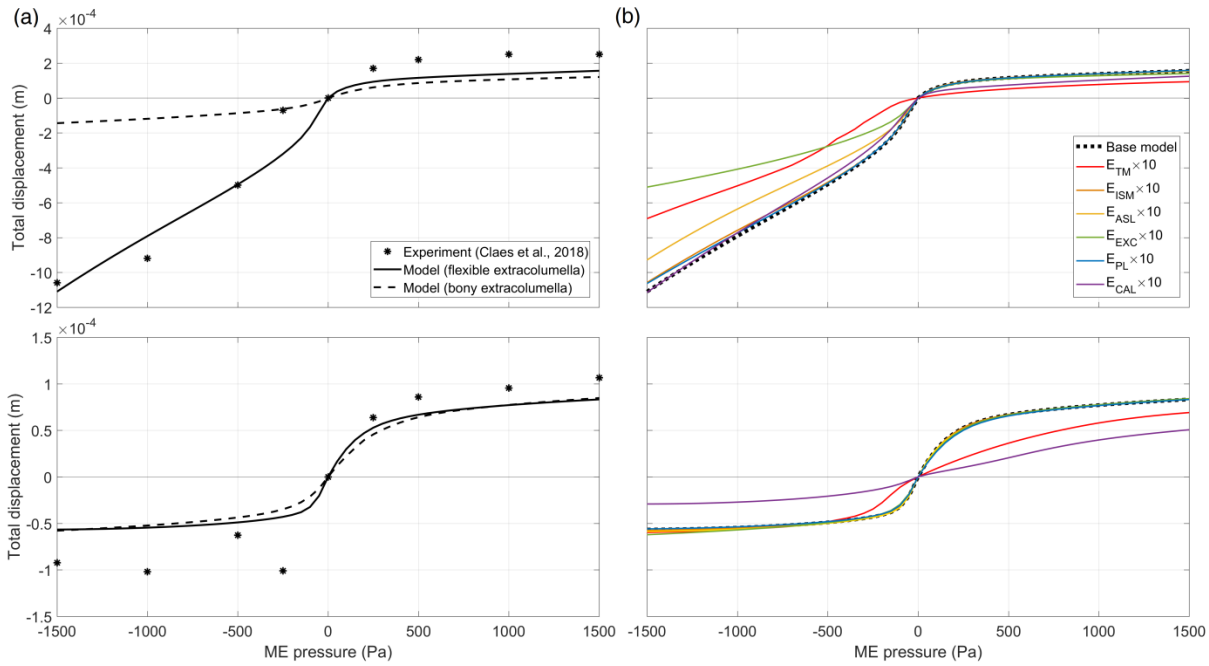

Figure 3. Total displacement of the umbo (top) and the footplate (bottom) as a function of middle-ear pressure. (a) The result of the normal model with flexible extracolumella is compared to the result of another model with a simulated bony extracolumella and to the result of a single measurement (Claes et al., 2018). (b) Result of a sensitivity analysis after multiplying the Young's modulus of each individual soft-tissue component by 10. TM, tympanic membrane; ISM, infrastapedial membrane; ASL, ascending ligament; EXC, extracolumella; PL, Platner's ligament; CAL, columellar annular ligament.

3.1.1.1 The base model

When the extracolumella is considered flexible, with a Young's modulus of 3 MPa as indicated in Table 1, the model is able to qualitatively reproduce one of the measurements in Claes et al. (2018), showing much larger inward umbo displacements at negative pressure (~1.1 mm at –1.5 kPa) than outward displacements at positive pressure (~0.2 mm at +1.5 kPa) as depicted in the upper panel of Fig. 3 (a). This asymmetry is not observed in the results of the footplate displacement in the lower panel of Fig. 3 (a), where displacements between both pressure sides are similar. At negative pressure, displacements are greatly reduced from the umbo to the footplate, with a ratio between umbo and footplate of 19.6 at –1.5 kPa. At +1.5 kPa the ratio only amounts to 1.9.

To demonstrate the importance of flexibility of the extracolumella, the model was calculated again in which the extracolumella was simulated as completely ossified, with a Young's modulus of 14.1 GPa like the bony

columella. This adaptation to the model drastically reduces the large umbo displacements at negative middle-ear pressure and almost completely removes the asymmetry in the umbo displacement curve (upper panel, Fig. 3 (a)). The change in the displacement curve of the footplate is much smaller (lower panel, Fig. 3 (a)). The main difference with the flexible model is that the shape of the footplate curve looks slightly less nonlinear, as the slope of the curve remains more stable. When considering the ratio of umbo-to-footplate displacement, it is found that the reduction in displacement from the umbo to the footplate at negative pressure is much smaller with bony than with flexible extracolumella, reaching a ratio of 2.5.

3.1.1.2 Sensitivity analysis

The results of the sensitivity analysis with respect to the soft-tissue Young's moduli are shown in Fig. 3 (b). For the umbo displacement (upper panel, Fig. 3 (b)), the Young's moduli of the tympanic membrane, extracolumella and ascending ligament have the highest influence at negative pressure. Between 0 and –0.5 kPa, the increased tympanic-membrane stiffness has the highest effect on the reduced umbo displacement, while between –0.5 and –1.5 kPa the influence of the extracolumella stiffness is highest. Other soft-tissue structures have only minor influence in this pressure regime. For positive pressure, the increased tympanic-membrane stiffness has the highest effect on the reduced umbo displacement overall, and the annular-ligament stiffness has the second to highest effect. The other structures again have minor influence in this pressure regime.

For the displacement of the footplate (lower panel, Fig. 3 (b)), the increased annular-ligament stiffness has the highest influence overall, reducing the displacement, and the tympanic-membrane stiffness has the second to highest effect between –0.5 and +1.5 kPa. For negative pressures between –0.5 and –1.5 kPa, the increased stiffness of the extracolumella, tympanic membrane and ascending ligament lead to a small (negative) increase of the footplate displacement. At –1.5 kPa the effect is the highest for the increased stiffness of the extracolumella, but when the extracolumella is modeled as bony with an even higher stiffness (E = 14.1 GPa) (lower panel, Fig. 3 (a)), the change in footplate displacement at –1.5 kPa is smaller.

3.1.2 Displacements of the columellar apparatus

Figure 4 shows the displacements of the columella and extracolumella in the model for different positive and negative pressures in the middle ear.

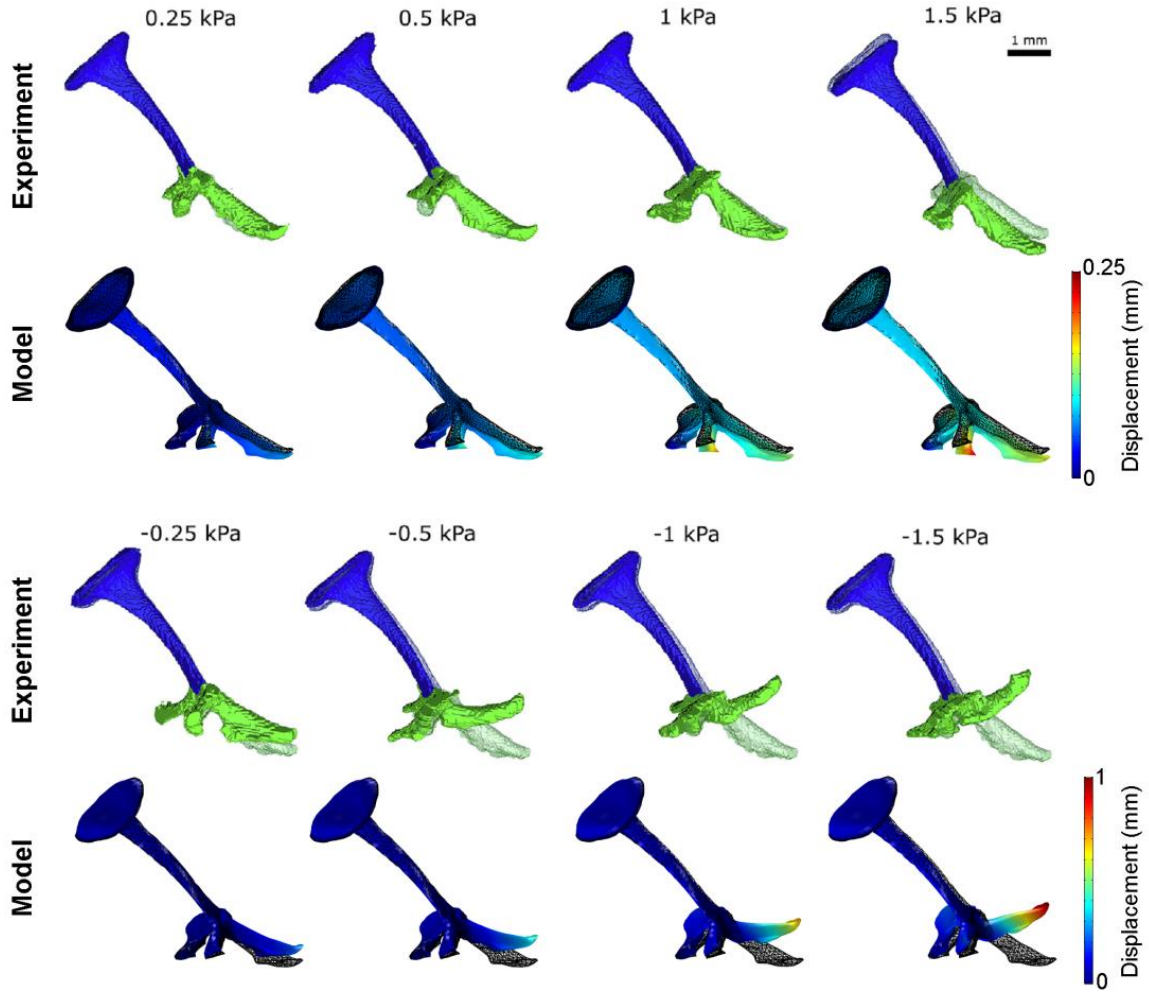

Figure 4. Total displacement of the columellar apparatus for different positive and negative middle-ear pressures (ventro-anterior view). Results of the normal model are compared to the results of a single measurement (Claes et al., 2018). For the experimental result, the deformed condition is shown in opaque and the resting condition in transparent. For the model, the deformed condition is given by the structure with superimposed color scale showing the total displacement, and the resting condition is given by the meshed structure. The tympanic membrane and Platner's ligament are not shown.

For positive middle-ear pressures, as depicted in the upper two rows of Fig. 4 for the measurement and the model, the columellar apparatus follows the gradual outward displacement of the tympanic membrane (not shown) in a similar fashion to one of the measurements in Claes et al. (2018). The maximal displacement of the umbo is around 0.2 mm at +1.5 kPa. No meaningful deformation of the extracolumella is observed.

In the case of negative middle-ear pressures, as shown in the lower two rows of Fig. 4, the distal end of the extrastapedius shows a large inward displacement to follow the large displacements of the tympanic membrane, with a maximal umbo displacement of around 1 mm at –1.5 kPa. However, this displacement is not penetrated further to the footplate because of bending in the extracolumella, which is made of compliant material. The

bending occurs in the extrastapedius in a zone just distal to the location where the three arms of the extracolumella join together.

3.2 The middle ear with modified tympanic-membrane cone

3.2.1 Umbo and footplate displacement

The results of umbo and footplate displacement for the models with adapted tympanic-membrane geometry are shown in the upper and lower panel of Fig. 5, respectively.

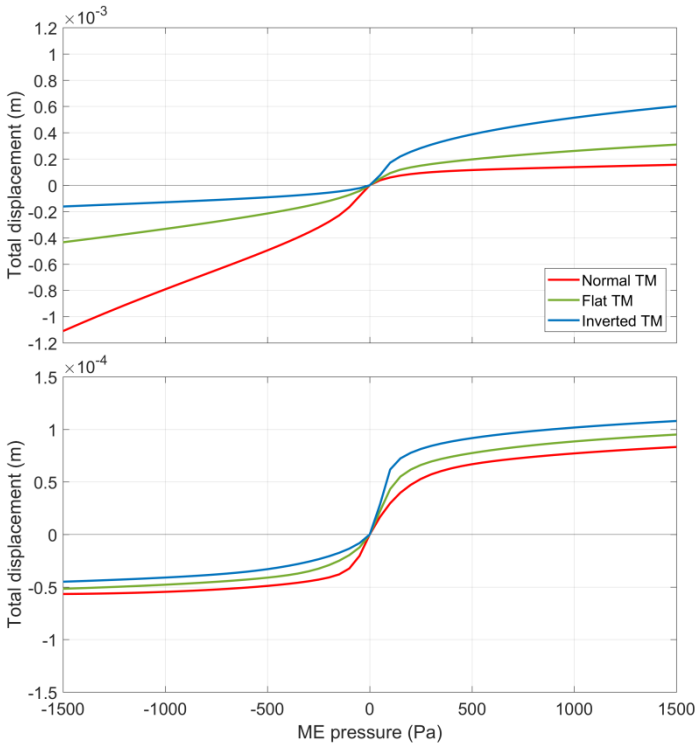

Figure 5. Total displacement of the umbo (top) and footplate (bottom) as a function of middle-ear pressure for the models with three different tympanic-membrane (TM) geometries.

For the model with flat tympanic membrane (green curves in Fig. 5) it is observed that the displacements of the umbo (upper panel) and footplate (lower panel) decrease at negative pressure and increase at positive pressure relative to the model with normal membrane. The original asymmetry in umbo displacement almost completely vanishes, showing almost equal displacements at positive and negative pressure. As such, this result suggests the importance of the tympanic-membrane cone shape on umbo displacement asymmetry. For the footplate the asymmetry increases, presenting larger displacements at positive than at negative pressure. When considering the umbo-to-footplate displacement ratio at negative pressure, it is noticed that the reduction of displacement from umbo to footplate is not as large for the flat as the normal membrane, with a ratio value of 8.4

at –1.5 kPa. For positive pressure, on the other hand, the reduction is greater when the membrane is flat, having a ratio of 3.3 at +1.5 kPa.

For the model with inverted tympanic membrane (red curves in Fig. 5), the changes in shape of the displacement curves evolve even further; the displacements additionally decrease at negative pressure and increase at positive pressure. The asymmetry of the umbo displacement (upper panel) reemerges but now with the largest displacements seen at positive pressure, similar to findings in mammals. The asymmetry of the footplate displacement (lower panel) that was obtained with the flat membrane develops even further to a displacement behavior that is typically seen in mammal ears. When considering the ratio of umbo-to-footplate displacement, we again observe that the reduction of displacement between umbo and footplate at negative pressure diminishes further down to a ratio 3.6 at –1.5 kPa, but at positive pressure it increases up to a ratio of 5.6 at +1.5 kPa.

3.2.2 Displacements of the columellar apparatus

Figure 6 compares displacements of the columellar apparatus in the models with modified tympanic-membrane geometry to the model with normal geometry. Displacements are shown for middle-ear pressures of +1.5 and –1.5 kPa.

For positive pressure, the columellar apparatus performs clear outward displacements for the three models, but the largest displacements are clearly seen with an inverted tympanic membrane. In the latter model the distal end of the extrastapedius displays a maximal outward displacement of 0.6 mm. This displacement goes along with considerable bending of the extracolumella, which for the normal model occurred at negative pressure. Bending again takes place in the extrastapedius just distal to the location where the three arms of the extracolumella meet, which is responsible for the fact that displacements are not substantially transferred to the footplate. At negative pressure, the displacements of the model with inverted membrane are much smaller than at positive pressure, which is opposite to the model with normal tympanic membrane where the maximal displacement occurred at negative pressure.

For the model with a flat tympanic membrane, the displacements appear to be about equally large for positive and negative pressure, besides being in opposite direction. Bending of the extracolumella occurs for both pressure conditions, but is less pronounced than in the models with a normal membrane (at negative pressure) and an inverted membrane (at positive pressure).

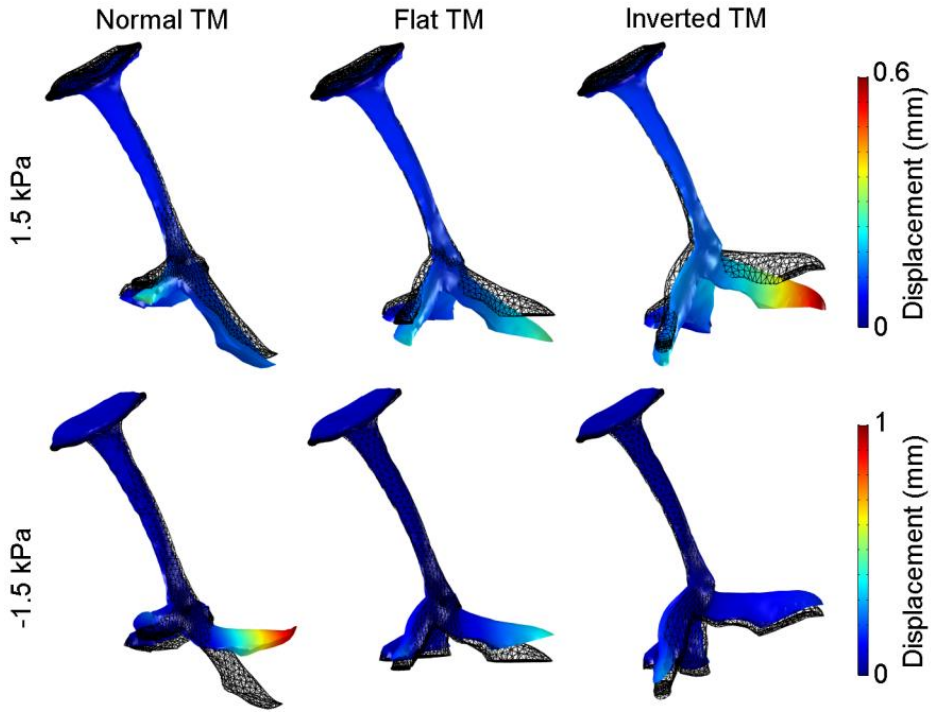

Figure 6. Total displacement of the columellar apparatus under positive and negative middle-ear pressure of 1.5 kPa for the models with three different tympanic-membrane (TM) geometries (ventro-anterior view).

4. Discussion

4.1 Orientation of the tympanic-membrane cone

4.1.1 Geometry of the columellar complex

When changing the orientation of the tympanic-membrane cone, the extracolumella was allowed to deform in such a way that the angle between the columellar shaft and the base plane of the membrane was preserved. However, this operation changed the angle between the columellar shaft and the extrastapedius, which may have influenced the results. Another possibility would be to retain the angle between the columellar shaft and extrastapedius while allowing the angle between the columellar shaft and the base plane of the membrane to deviate. However, this action would lead to a wrong position and orientation of the oval window and inner ear, and would also require a deformation of the extracolumella that may influence the results. The problem of deforming the extracolumella might be avoided by removing the side arms of the extracolumella (the infra- and suprastapedius) in both the normal, flat and inverted model. However, these arms are important to permit a piston-like motion of the columella and avoid tilting, as explained by von Békésy (1949). As a consequence, differences between the presented results may not be due to the altered orientation of the membrane alone but may also be partially related to the adjusted geometry of the columellar complex.

4.1.2 Umbo displacements

In Fig. 3 we observed a substantial asymmetry in the displacement curve of the umbo for the normal middle ear. Interestingly, the asymmetry is opposite to what is typically observed in mammal ears, such as human (e.g. Hüttenbrink, 1988; Dirckx and Decraemer, 1991; Murakami et al., 1997), gerbil (Dirckx and Decraemer, 2001) and rabbit (Dirckx et al., 2006). In these studies, the observed outward umbo displacements at positive middle-ear pressure were larger than the inward displacements at negative pressure, and the relative difference between the two pressure conditions was smaller than in the chicken. The model results presented in Fig. 5 and 6 suggest that this dissimilarity is related to the opposite orientation of the tympanic-membrane cone between birds and mammals. However, the asymmetry vanished when the extracolumella was modeled with the stiffness of bone. The nonlinear static displacements of the umbo and footplate were studied in human by Wang et al. (2007) and Ihrle et al. (2013) with finite-element simulations, which could both confirm the asymmetry in umbo displacement. Ihrle et al. (2013) showed that the asymmetry was also present when only geometric nonlinearity was taken into account, while disregarding material nonlinearity of the tympanic membrane. The asymmetry of deformation versus load can also be affected by the viscoelastic behavior of middle-ear tissues, and especially the tympanic membrane (e.g., Cheng et al., 2007; Motallebzadeh et al., 2013). The asymmetry of the displacement depends on the loading direction (i.e., increasing or decreasing pressure), which is known as hysteresis. Such behavior was also observed for the tympanic-membrane volume displacement in tympanometry measurements (e.g., Gaihede and Kabel, 2000). This effect is not captured by the current models, which only account for the elastic behavior due to static loading. In the present models, the displacement asymmetry with loading direction is probably not only due to the conical shape, but also to the curvature of the membrane. Funnell and Laszlo (1978) found that membrane curvature affects the umbo and peak displacement of the membrane in a linear elastic model of the cat middle ear. It can be expected that geometric nonlinearity will yield an asymmetric compliance of the curved membrane depending on the loading direction, such as for a curved beam that shows a different deflection behavior dependent on the direction of a transverse load.

4.1.3 Footplate displacements

For the footplate, the asymmetry in the displacement curves was much smaller, with slightly larger displacement values at positive than at negative middle-ear pressure. In the measurements of Claes et al. (2018) a small asymmetry was observed in the displacement curves, with on average the largest displacements seen at negative pressure. However, due to the strong overlapping of the large error bars between positive and negative middle-ear pressure, the footplate displacement of an individual ear has no strong preference towards positive or

negative pressure, as was the case for the single measurement shown in Fig. 3 (Claes et al., 2018). In Muyshondt et al. (2018) the average footplate displacement in ostrich was larger at positive than at negative middle-ear pressure of 1 kPa, but again with overlapping standard deviations. In mammals the footplate displacement showed a preference for positive middle-ear pressures; in rabbit the asymmetry between positive and negative pressure was substantial (Dirckx et al., 2006), but in human it was much smaller (Hüttenbrink, 1988; Murakami et al., 1997).

4.1.4 Function of the tympanic-membrane cone

The effect of changing the orientation of the tympanic-membrane cone (and adapting the geometry of the columellar complex accordingly) on the asymmetry of the umbo displacement curve is clear, as demonstrated by the different models in the current work, but what is the advantage of an outward-pointing conical membrane? In the lower panel of Fig. 5 it was seen that the displacement curve of the footplate is more symmetrical with an outward-pointing membrane than with a flat or an inward-pointing membrane; the latter two models present higher outward footplate displacements at positive middle-ear pressure, and the maximal footplate displacement overall is larger than for an outward-pointing membrane, so it appears that the normal model displays a superior protective performance. Because the displacement behavior of the footplate shows some variation between specimens (Claes et al., 2018), and because the differences between the models with different membrane cone orientations may be partially due to the adjusted geometry of the columellar complex, further experimental and model testing is needed to confirm this result. Another probable advantage of the curved conical membrane shape is related to transmission of sound, as investigated in mammal ears (Funnell and Laszlo, 1978; Koike et al., 2001; Fay et al., 2006). It was found that a normal curved conical membrane resulted in the most optimal sound transmission. The function of the membrane is to match the low impedance of air to the high impedance of the malleus to be able to transmit vibration energy to the umbo. If the membrane is flat, it is too flexible and cannot use its in-plane stiffness to resist loads perpendicular to the plane of the membrane, but only its low bending stiffness; in such case, the membrane matches the impedance of air, but not of the malleus, and it will be unable to drive the umbo. When the membrane has a curved conical shape, the less conical outer portions of the membrane will match the low impedance of air, while the inner conical portions will better match the high impedance of the malleus due to the membrane's in-plane stiffness in the direction of the radial fibers, so it will be better able to make the umbo vibrate. Theoretically, this reasoning holds both for an outward and an inward curved conical membrane. To understand the role of the outward-pointing membrane cone on the acoustic function of the middle ear, further modeling of sound transmission in the bird middle ear is needed.

4.2 *Flexibility of the single-ossicle ear*

The role of flexibility in the middle ear of vertebrates was summarized by Mason and Farr (2013). The conclusion from their work was that flexibility likely functions to buffer the ear against high-amplitude quasi-static pressure changes, although it will generally reduce sound transmission through the middle ear. More recently, it was argued by Gottlieb et al. (2018) that middle-ear flexibility in human reduces peak amplitudes of impulsive sounds to protect the sensory cells in the cochlea. In mammals, flexibility is mainly associated with the synovial joints between the ossicles, which do not exist in birds. Middle-ear flexibility in birds is usually associated with structures coupling the columella to the tympanic membrane, as explained further below.

4.2.1 Flexibility in the literature

In the literature, several studies exist that describe the displacements of the columellar apparatus in birds, which mostly emphasize the importance of flexibility in the intracolumellar connection. Smith (1904) observed the great flexibility between the columella and extracolumella, which was due to the cartilaginous neck which unites them. Pohlman (1921) described the existence of three hinges in the columellar apparatus of the chicken, which describe the motion of the extracolumella as a whole or bending motions taking place in the extracolumella: (1) the columellar hinge at the connection between the columella and extracolumella, (2) the suprastapedial hinge at the connection between the suprastapedius and the tympanic membrane, and (3) the extrastapedial hinge in extrastapedius just distal to the confluence of the supra- and infrastapedius. The last hinge corresponds to the bending zone observed in the current study. Mills and Zhang (2006) studied the qualitative quasi-static behavior of the columellar apparatus in four bird species (glaucous gull, rock dove, gannet and pheasant) by applying static pressures from -10 to +10 Pa in the ear canals. They concluded that the off-center attachment of the extracolumella to the tympanic membrane and the flexion of the joint between the columella and extracolumella results in rocking motion of the footplate rather than a pure piston-like motion. It was postulated that this mechanism serves as protection to avoid excessive displacement of footplate in the scala vestibuli. Arechvo et al. (2013) studied the quasi-static displacements of the ostrich middle ear under positive pressures in the ear canal up to 2 kPa, and found a buckling movement in the chain between the cartilaginous extracolumella and bony columella, which was also identified as a protective mechanism. Muyshondt et al. (2018) observed a bending of the extracolumella in the ears of five ostrich heads under negative middle-ear pressure of 1 kPa. In one specimen buckling of the intracolumellar connection took place, leading to rocking motion of the footplate.

4.2.2 Flexibility in the present study

In the current work a modeling approach was used in an attempt to describe the quasi-static measurements of Claes et al. (2018) in chicken. From Fig. 4 it was deduced that large displacements of the umbo at negative middle-ear pressure are permitted by flexibility of the extracolumella. Due to this flexibility, the extrastapedius performs a substantial bending motion, which reduces displacements from the umbo to the footplate. When the extracolumella is modeled as a stiff bony material instead, a larger relative portion of the umbo displacement is transferred to the footplate. However, because the displacements of the umbo also decrease substantially, the footplate displacement curve is similar to the curve obtained with flexible extracolumella (lower panel, Fig. 3 (a)). Footplate displacements are more influenced by the flexibility of the tympanic membrane and annular ligament (lower panel, Fig. 3 (b)). An alternative explanation for the flexible nature of the extracolumella is related to the coupling with the tympanic membrane. A stiff extracolumella causes a higher stress in the membrane at the connections with the processes of the extracolumella and in the central parts of the membrane when there is a pressure gradient across it (not shown). Hence, an inflexible extracolumella could make decoupling or rupture of the membrane more likely, or it could lead to a reduction of sound transmission when the membrane is subjected to a quasi-static pressure gradient.

The flexibility of the extracolumella may also be important for sound transmission. Some flexibility may be needed to bridge the acoustic impedance mismatch between the tympanic membrane and the bony columella that would exist with a fully ossified single-ossicle apparatus; a compliant extracolumella probably enhances the coupling between the vibrations of the membrane and the columellar apparatus at low frequencies, but possibly also explains the poor sound transmission and hearing at high frequencies in birds (Manley, 1990; Mason and Farr, 2013). This hypothesis should be tested by modeling the harmonic response of the bird middle ear to sound-pressure stimulation.

4.3 Physiological pressures and Eustachian-tube function

In the present work, the effect of positive and negative middle-ear pressures up to 1.5 kPa was investigated, similar to the measurements of Claes et al. (2018). However, measurements of Larsen et al. (1997) showed that middle-ear pressure steadily grows negative in awake birds over a period of seconds to minutes, but is reset once it reaches –20 to –40 Pa, probably by passively or actively opening the Eustachian tube. In chickens, spontaneous venting occurred around –250 Pa during anesthesia (Larsen et al., 2016). Such physiological

pressures are smaller than the pressures investigated here, but presumably these are more frequently encountered by many flying birds.

5. Conclusion

The nonlinear quasi-static displacement of the umbo is highly asymmetrical in the chicken, showing much larger displacements at negative than at positive middle-ear pressure. To explain this behavior, the extracolumella needs to be made of flexible material. The extracolumella shows a great bending motion, which reduces displacements from the umbo to the footplate. A stiff extracolumella allows for a greater relative transfer of displacement from umbo to footplate, but at the same time it reduces the absolute umbo displacement. Hence, the eventual footplate displacement remains almost unaffected by changes in stiffness of the extracolumella. The asymmetry of the umbo displacement curve is opposite to the asymmetry observed in mammals. The present results suggest that this difference in asymmetry is caused by the opposite orientation of the tympanic-membrane cone of birds and mammals. The asymmetry in the displacement of the footplate is smaller, but increases when we use a flat or inverted membrane geometry, showing a gain of displacement at positive pressure and a loss at negative pressure. However, these results may be partially due to the adaptations in the geometry of the columellar complex. The role of flexibility and membrane cone orientation on sound transmission in birds remains to be investigated.

Conflicts of interest

None.

Contributors

P.G.G.M. created the finite-element models, analyzed the data and wrote the manuscript. J.J.J.D. and P.A. participated in the design of the study. All authors gave their final approval for publication.

Acknowledgments

We thank R. Claes en J. Goyens for their help with the micro-CT scanning. We also acknowledge the funding agency, the Research Foundation – Flanders (FWO), for their financial support, grant nr. 11T9318N.

References

Arechvo, I., Zahnert, T., Bornitz, M., Neudert, M., Lasurashvili, N., Simkunaite-Rizgeliene, R., 2013. The ostrich middle ear for developing an ideal ossicular replacement prosthesis. Eur. Arch. Otorhinolaryngol. 270, 37–44. https://doi.org/10.1007/s00405-011-1907-1.

Buytaert, J.A.N., Goyens, J., De Greef, D., Aerts, P., Dirckx, J.J.J., 2014. Volume shrinkage of bone, brain and muscle tissue in sample preparation for micro-CT and light sheet fluorescence microscopy (LSFM). Microsc. Microanal. 20, 1208–1217. https://doi.org/10.1017/S1431927614001329.

Cheng, T., Dai, C., Gan, R.Z., 2007. Viscoelastic properties of human tympanic membrane. Ann. Biomed. Eng. 35, 305–314. https://doi.org/10.1007/s10439-006-9227-0.

Claes, R., Muyshondt, P.G.G., Van Assche, F., Van Hoorebeke, L., Aerts, P., Dirckx, J.J.J., 2018. Eardrum and columella displacement in single ossicle ears under quasi-static pressure variations. Hear. Res. 365, 141–148. https://doi.org/10.1016/j.heares.2018.05.012.

Dirckx, J.J.J., Decraemer, W.F., 1991. Human tympanic membrane deformation under static pressure. Hear. Res. 51, 93–105. https://doi.org/10.1016/0378-5955(91)90009-X.

Dirckx, J.J.J., Decraemer, W.F., 2001. Effect of middle ear components on eardrum quasi-static deformation. Hear. Res. 157, 124–137. https://doi.org/10.1016/S0378-5955(01)00290-8.

Dirckx, J.J.J., Buytaert, J.A.N., Decraemer, W.F., 2006. Quasi-static transfer function of the rabbit middle ear, measured with a heterodyne interferometer with high-resolution position decoder. JARO 7, 339–351. https://doi.org/10.1007/s10162-006-0048-5.

Dirckx, J.J.J., Decraemer, W.F.S., 1992. Area change and volume displacement of the human tympanic membrane under static pressure. Hear. Res. 62, 99–104. https://doi.org/10.1016/0378-5955(92)90206-3.

Elner, A., Ingelstedt, S., Ivarsson, A., 1971. The elastic properties of the tympanic membrane system. Acta Otolaryngol. 71, 397–403. https://doi.org/10.3109/00016487109122499.

Fay, J.P., Puria, S., Steele, C.R., 2006. The discordant eardrum. PNAS 103, 19743–19748. https://doi.org/10.1073/pnas.0603898104.

Filogamo, G., 1949. Recherches sur la structure de la membrane du tympan chez les differents vertebres. Acta Anat. 7, 248–272. https://doi.org/10.1159/000140387.

Funnell, W.R.J., Laszlo, C.A., 1978. Modeling of the cat eardrum as a thin shell using the finite-element method. J. Acoust. Soc. Am. 63, 1461–1467. https://doi.org/10.1121/1.381892.

Gaihede, M., Kabel, J., 2000. The normal pressure-volume relationship of the middle ear system and its biological variation. In: Rosowski, J.J., Merchant, S.N. (Eds.), The Function and Mechanics of Normal, Diseased and Reconstructed Middle Ears, pp. 59–70. The Hague: Kügler Publications.

Gottlieb, P.K., Vaisbuch, Y., Puria, S., 2018. Human ossicular-joint flexibility transforms the peak amplitude and width of impulsive acoustic stimuli. J. Acoust. Soc. Am. 143, 3418. https://doi.org/10.1121/1.5039845.

Herrmann, G., Liebowitz, H., 1972. Mechanics of bone fracture. In: Liebowitz, H. (Ed.), Fracture of Nonmetals and Composits. New York: Academic Press, pp. 771–840. https://doi.org/10.1016/b978-0-12-449707-8.50014-2.

Hüttenbrink, K.B., 1988. The mechanics of the middle-ear at static air pressures: the role of the ossicular joints, the function of the middle-ear muscles and the behavior of stapedial prostheses. Acta Otolaryngol. 105, 1–35. https://doi.org/10.3109/00016488809099007.

Ihrle, S., Lauxmann, M., Eiber, A., Eberhard, P., 2013. Nonlinear modelling of the middle ear as an elastic multibody system – Applying model order reduction to acousto-structural coupled systems. J. Comput. Appl. Math. 246, 18–26. https://doi.org/10.1016/j.cam.2012.07.010.

Kirikae, J., 1960. The structure and function of the middle ear. Tokyo, University of Tokyo Press.

Koike, T., Wada, H., Kobayashi, T., 2001. Effect of depth of conical-shaped tympanic membrane on middle-ear sound transmission. JSME Int. J. Ser. C 44, 1097–1102. https://doi.org/10.1299/jsmec.44.1097.

Larsen, O.N., Dooling, R.J., Ryals, B.M., 1997. Roles of intracranial air pressure in bird audition. In: Lewis, E.R., Long, G.R., Lyon, R.F., Narins, P.M., Steele, C.R., Hecht-Poinar, E. (Eds.), Diversity in Auditory Mechanisms, pp. 11–17. Singapore: World Scientific. https://doi.org/10.1142/9789814531023.

Larsen, O.N., Christensen-Dalsgaard, J., Jensen, K.K., 2016. Role of intracranial cavities in avian directional hearing. Biol. Cybern. 110, 319–331. https://doi.org/10.1007/s00422-016-0688-4.

Maftoon, N., Funnell, W.R.J., Daniel, S.J., Decraemer, W.F., 2015. Finite-element modelling of the response of the gerbil middle ear to sound. JARO 16, 547–567. https://doi.org/10.1007/s10162-015-0531-y.

Manley, G.A., 1990. Overview and outlook. In: Manley, G.A. (Ed.), Peripheral Hearing Mechanisms in Reptiles and Birds. Zoophysiology. Springer-Verlag, Berlin, Heidelberg, pp. 253–273. https://doi.org/10.1007/978-3-642-83615-2_14.

Mason, M.J., Farr, M.R.B., 2013. Flexibility within the middle ears of vertebrates. J. Laryngol. Otol. 127, 2–14. https://doi.org/10.1017/S0022215112002496.

Mills, R., Zhang, J., 2006. Applied comparative physiology of the avian middle ear: the effect of static pressure changes in columellar ears. J. Laryngol. Otol. 120, 1005–1007. https://doi.org/10.1017/S0022215106002581.

Motallebzadeh, H., Charlebois, M., Funnell, W.R.J., 2013. A non-linear viscoelastic model for the tympanic membrane. J. Acoust. Soc. Am. 134, 4427–4434. https://doi.org/10.1121/1.4828831.

Motallebzadeh, H., Maftoon, N., Pitaro, J., Funnell, W.R.J., Daniel, S.J., 2017. Finite-element modeling of the acoustic input admittance of the newborn ear canal and middle ear. JARO 18, 25–48. https://doi.org/10.1007/s10162-016-0587-3.

Murakami, S., Gyo, K., Goode, R.L., 1997. Effect of middle ear pressure change on middle ear mechanics. Acta Otolaryngol. 117, 390–395. https://doi.org/10.3109/00016489709113411.

Muyshondt, P.G.G., Soons, J.A.M., De Greef, D., Pires, F., Aerts, P., Dirckx, J.J.J., 2016a. A single-ossicle ear: acoustic response and mechanical properties measured in duck. Hear. Res. 340, 35–42. https://doi.org/10.1016/j.heares.2015.12.020.

Muyshondt, P.G.G., Aerts, P., Dirckx, J.J.J., 2016b. Acoustic input impedance of the avian inner ear measured in ostrich (Struthio camelus). Hear. Res. 339, 175–183. https://doi.org/10.1016/j.heares.2016.07.009.

Muyshondt, P.G.G., Claes, R., Aerts, P., Dirckx, J.J.J., 2018. Quasi-static and dynamic motions of the columellar footplate in ostrich (Struthio camelus) measured ex vivo. Hear. Res. 357, 10–24. https://doi.org/10.1016/j.heares.2017.11.005.

Norberg, R.Å., 1978. Skull asymmetry, ear structure and function, and auditory localization in Tengmalm's owl, Aegolius funereus (Linné). Phil. Trans. R. Soc. B 282, 325–410. https://doi.org/10.1098/rstb.1978.0014.

Pohlman, A.G., 1921. The position and functional interpretation of the elastic ligaments in the middle-ear of Gallus. J. Morphol. 35, 228–262. https://doi.org/10.1002/jmor.1050350106.

Smith, G., 1904. The middle ear and columella of birds. Q. J. Microsc. Sci. 48, 11–22.

Starck, J.M., 1995. Comparative anatomy of the external and middle ear of palaeognathous birds. Adv. Anat. Embryol. Cell Biol. 131, 1–137. https://doi.org/10.1007/978-3-642-79592-3.

Thomassen, H.A., Gea, S., Maas, S., Bout, R.G., Dirckx, J.J.J., Decraemer, W.F., Povel, G.D.E., 2007. Do Swiftlets have an ear for echolocation? The functional morphology of Swiftlet's middle ears. Hear. Res. 225, 25–37. https://doi.org/10.1016/j.heares.2006.11.013.

von Békésy, G., 1949. The structure of the middle ear and the hearing of one's own voice by bone conduction. J. Acoust. Soc. Am. 21, 217–232. https://doi.org/10.1121/1.1906501.

Wang, X., Cheng, T., Gan, R.Z., 2007. Finite-element analysis of middle-ear pressure effects on static and dynamic behavior of human ear. J. Acoust. Soc. Am. 122, 906–917. https://doi.org/10.1121/1.2749417.